Short-range shock formation and coalescence in numerical simulation of broadband noise propagation

Micah R. Shepherd[a)]
Applied Research Laboratory, The Pennsylvania State University, P.O. Box 30, State College, Pennsylvania 16804

Kent L. Gee
Department of Physics and Astronomy, Brigham Young University, N-243 ESC, Provo, Utah 84602

Mark S. Wochner
Applied Research Laboratories, The University of Texas at Austin, P.O. Box 8029, Austin, Texas 78713

(Received 19 January 2009; revised 9 September 2009; accepted 10 September 2009)

The number of jet and rocket noise studies has increased in recent years as researchers have sought to better understand aeroacoustic source and radiation characteristics. Although jet and rocket noise is finite-amplitude in nature, little is known about the existence of shock formation and coalescence close to the source. A numerical experiment is performed to propagate finite-amplitude noise and determine the extent of the nonlinearity over short distances with spherical spreading. The noise is filtered to have a haystack shape in the frequency domain, as is typical of such sources. The effect of the nonlinearity is compared in both the temporal and frequency domains as a function of distance. Additionally, the number of zero-crossings and overall sound pressure level is compared at several distances. The results indicate that the center frequency plays a particularly important role in the amount of coalescence and spectral redistribution that occurs. The general applicability of these results to actual near-field finite-amplitude jet and rocket noise experiments is also presented. © *2009 Acoustical Society of America.* [DOI: 10.1121/1.3243466]

PACS number(s): 43.25.Cb [RR] Pages: 2886–2893

I. INTRODUCTION

The propagation of intense random acoustic noise has important applications in the present day. Military jet aircraft and launch vehicle technologies are rapidly advancing to meet new challenges, often causing such aircraft to produce higher thrust and consequently high noise levels which propagate nonlinearly. Characterization of these high-amplitude aeroacoustic sources is a necessary part of predicting structural vibration of the vehicle as well as the impact of noise on the surrounding community and environment.

Early experimental studies of noise produced by jets and rockets[1–6] began in the 1950s. The effort to characterize and ultimately predict far-field noise propagation has continued to the present with a wave of recent research.[7–13] These studies, along with other analytical studies (see, e.g., Tam *et al.*[14]), have established the spectral characteristics common to jet and rocket noise, namely, an increase according to f^2 up to some center frequency followed by a decrease according to f^{-2}. This spectral shape is commonly referred to as a haystack spectrum and is a result of the large scale turbulent structure of the jet.[15] Note that waveforms with haystack spectra and waveforms with flat, white-noise spectra with the same rms levels will have appreciably different peak pressures. The haystack-based waveform has greater peak pressures because the relative levels around the center frequency must be greater to produce the same rms level.

Nonlinear effects in the propagation of jet noise propagation were first studied by Morfey and Howell[16] and more recently by Gee *et al.*[7] McInerny and Ölçmen[17] also showed evidence of nonlinear propagation in rocket noise. Published overall sound pressure levels (OASPLs) of military jet aircraft noise (F-22A Raptor) are 143 dB at 23 m,[7] while published Titan IV rocket noise levels are 140 dB at 820 m.[17] By removing spreading back to 1 m, these values are approximately 170 dB for the jet aircraft and 198 dB for the rocket. All levels here and in the rest of the article are referenced to 20 μPa. Although spherical spreading will not hold at 1 m due to the spatially extended nature of the turbulence, these numbers are nevertheless illustrative of the extremely high amplitudes near the jet or rocket noise source. Acoustical measurements of static, horizontally fired four-segment reusable solid rocket motors (like those used on Space Shuttles) reveal levels that are likely slightly lower than the Titan IV.[10] However, note that the proposed ARES I and ARES V vehicles will use 5-segment and 5.5-segment versions of the current four-segment motors, which may result in a slight increase in level.

The first laboratory study of intense broadband noise propagation was performed by Pestorius and Blackstock.[18] Band-limited broadband noise was propagated down a 29.3 m (96 ft) tube and compared to numerically propagated noise. The algorithm and experiment showed good agreement of shock formation and propagation at sound pressure levels up to 160 dB. Other laboratory experiments of finite-amplitude noise propagation are summarized by Gurbatov and Rudenko.[19]

[a)]Author to whom correspondence should be addressed. Electronic mail: mrs30@psu.edu

Many numerical studies of nonlinear propagation have also been performed,[20–22] though only a few have studied the nonlinear propagation of noise. As mentioned, Pestoruis and Blackstock developed a numerical solution of the generalized Mendouse–Burgers equation and studied one-dimensional propagation of band-limited finite-amplitude noise. However, this study did not include geometrical spreading or discuss the effects of the initial spectral shape of the waveform. To more accurately model the actual propagation of jet noise through the atmosphere, the Pestorius and Blackstock algorithm was further developed to include spherical spreading by Blackstock.[23] Most recently, Gee *et al.*[7] made further developments to the algorithm and performed in-depth studies of far-field jet noise propagation according to engine status and angle. The input waveforms used in the latter study were measured data recorded 23 m (75.4 ft) from an F-22A Raptor.

When including spherical spreading in a calculation, there will be substantially less waveform steepening and shock formation compared to the one-dimensional propagation scenario studied by Pestorius and Blackstock.[18] Because of this, they postulated that significant low frequency buildup due to the loss of zero-crossings resulting from shock coalescence will not occur in practical applications. When spherical spreading is included in the finite-amplitude propagation of noise, they argued that spreading losses will prevent low frequency buildup from being significant.

The shock formation distance using weak shock theory[24] for monofrequency waves seems to concur with the postulation from Pestorius and Blackstock since geometrical spreading requires much longer distances for significant nonlinear distortion and shock formation to occur than is necessary for an equivalent non-spreading case. This idea is illustrated well when the shock formation distance ($\bar{r}$) for monofrequency spherical waves is expressed in terms of shock formation distance ($\bar{x}$) for non-spreading monofrequency waves.

$$\bar{r} = r_0 e^{(1/\beta\epsilon k r_0)} = r_0 e^{(\bar{x}/r_0)}. \tag{1}$$

Here, r_0 is some distance where the waveform is known, β is the coefficient of nonlinearity, ϵ is the acoustic Mach number, and k is the acoustic wavenumber. The definition of the narrowband noise shock formation distance is similar to Eq. (1), except that the rms pressure is used as opposed to the maximum pressure.[19]

Care must be taken when using the shock formation distance of narrowband noise to gain insight into the behavior of nonlinear propagation of broadband noise since the sound pressure level is based on the rms pressure and does not tell the entire story. For a Gaussian process, the instantaneous pressure will be greater than the rms pressure 31.7% of the time. Furthermore, the actual pressure will be 6 dB higher than rms (i.e., greater than 2 std from mean) 4.6% of the time and 9.5 dB higher than rms 0.3% of the time. Although this may seem inconsequential, for a 1 s recording of Gaussian noise sampled at 20 kHz there will likely be over 800 samples 6 dB higher than the rms pressure and 20 samples 9.5 dB higher than rms pressure. Therefore a broadband noise signal of finite amplitude will likely have waveform steepening and shock formation faster than estimates based on narrowband noise shock formation distances. The more important indicators of shock formation are the peak pressures (i.e., the extreme-valued pressures).

Supersonic jet and rocket noise, however, is not Gaussian distributed but has been shown to have an asymmetric distribution. McInerny[25] found rocket noise to exhibit nonzero skewness, while Petitjean *et al.*[26] and Gee *et al.*[27] found similar trends from model-scale and full-scale jet noise experiments, respectively. This indicates that there will likely be more extreme-valued pressures in jet and rocket noise than in a Gaussian process.

Once the extreme-valued pressures have propagated a distance sufficient to form shocks, the decay of the shock will no longer follow geometrical spreading, and the speed of the shock U_{sh} is dictated by weak shock theory[24] to be

$$U_{\mathrm{sh}} = c_0 + \beta \frac{p_a + p_b}{2\rho_0 c_0}, \tag{2}$$

where c_0 is the small signal sound speed, p_a is the pressure in front of the shock, p_b is the pressure behind the shock, and ρ_0 is the ambient fluid density. The shocks from these extreme-valued pressures may travel faster than other parts of the waveform and eventually overtake them, causing coalescence. Therefore, the extreme-valued pressures, which can easily be 8–10 dB greater than the rms pressure, will play an important role in the amount of shock coalescence.

Only a handful of studies have addressed shock coalescence either analytically or numerically. The Pestorius and Blackstock[18] algorithm predicted a downward shift in center frequency due to the loss of zero-crossing resulting from shock coalescence. Lighthill[28] performed an analytical study for conical shock waves, describing coalescence in terms of shock "bunchings," "unions," and "proness to form further unions." Khokhlova *et al.*[29] proposed a statistical characterization of shock coalescence using an analogy to kinetic theory of inelastic particles. However, it has not been experimentally determined if significant shock coalescence could occur near a military jet aircraft or launch vehicle.

Since our understanding of jet and rocket noise relies on measurements near the source, the question must be raised: Are nonlinear effects important in the short-range propagation of jet and rocket noise and if so, how will this influence typical characterization methods? Furthermore, how significant of a role does the center frequency play in the propagation? In this article, a numerical experiment is presented in which haystack noise waveforms at amplitudes similar to those expected near military aircraft and launch vehicles are propagated over short distances. This will shed insight into whether significant shock formation and coalescence can realistically occur close to a finite-amplitude jet or rocket noise source despite the spherical spreading. Once this is established, a simple linear reconstruction is performed to reveal the spectral changes in the waveform as a function of short-range propagation distance and center frequency.

II. PROPAGATION METHODS

The propagation algorithm used for this study was recently developed by Wochner[30] and builds off prior work by Sparrow and Raspet.[20] To outline the physics modeled in the propagation algorithm, the equation set and numerical methods used in this research will be briefly reviewed. A detailed derivation is found in Ref. 31.

The equation set is an extended Navier–Stokes equation set comprised of conservation equations. They are defined for spherical waves in one dimension as

$$\frac{\partial \rho}{\partial t} + \frac{\partial \rho u}{\partial r} + 2\frac{\rho u}{r} = 0, \tag{3}$$

$$\frac{\partial \rho u}{\partial t} + \frac{\partial \rho u^2}{\partial r} = -\frac{\partial p}{\partial r} + \mu_B \frac{\partial^2 u}{\partial r^2} + \mu \frac{\partial \phi_{rr}}{\partial r} - \frac{2\rho u^2}{r}, \tag{4}$$

$$\frac{\partial \rho s_{\mathrm{fr}}}{\partial t} + \frac{\partial \rho u s_{\mathrm{fr}}}{\partial r} = \sigma_s - \sum_{\nu} \frac{\rho}{T_\nu} c_{u\nu} \frac{DT_\nu}{Dt} + \frac{\partial}{\partial r}\left(\frac{\kappa}{T}\frac{\partial T}{\partial r}\right) - \frac{2\rho u s}{r}, \tag{5}$$

and

$$\frac{\partial \rho T_\nu}{\partial t} + \frac{\partial \rho u T_\nu}{\partial r} = \frac{\rho}{\tau_\nu}(T - T_\nu) - \frac{2\rho u T_\nu}{r}. \tag{6}$$

In the above equations, ρ is the total fluid density, u is the particle velocity, μ and μ_B are the shear and bulk viscosities, ϕ_{rr} is the rate of shear tensor, s_{fr} is the total frozen entropy, T is the total absolute temperature, κ is the coefficient of thermal conduction, $c_{v\nu}$ is the specific heat constant of the ν-type molecule, σ_s is the entropy source term, and T_ν and τ_ν are the apparent vibration temperature and relaxation time of the ν-type molecule.

To solve the equation set, the temporal and spatial variables are grouped together to form a matrix equation of this form

$$\frac{\partial \mathbf{w}}{\partial t} + \frac{\partial \mathbf{F}}{\partial r} = \mathbf{H}, \tag{7}$$

where $\mathbf{w}$ is a matrix of the time-dependent variables, $\mathbf{F}$ is a matrix of the r-dependent variables, and $\mathbf{H}$ is a matrix of the remaining source-like terms. The acoustic pressure p is then found using the van der Waals form of the equation of state,

$$p = c^2\left[(\rho - \rho_0) + \frac{\gamma - 1}{2\rho_0}(\rho - \rho_0)^2 + \frac{\rho\beta T}{c_p}(s_{\mathrm{fr}} - s_{\mathrm{fr}_0})\right], \tag{8}$$

which relates the acoustic pressure, density, and entropy of a perturbation, where the subscript "0" represents the ambient values. As noted by Wochner,[30] this Eqs. (3)–(6) are an extension of the Yano and Inoue[21] equation set in that thermoviscous and molecular relaxation losses are added to the Euler equations. Important to note is that no weak nonlinearity or far-field assumptions are made in the derivation of this equation set.

Equation (7) is solved using a weighted essentially nonoscillatory (WENO) scheme[32] in space and third-order Runge–Kutta scheme in time. The WENO scheme is able to stably propagate discontinuities and therefore will not go unstable when shocks with near infinite slopes form. More details regarding the implementation of the WENO scheme can be found in Ref. 30. Previous uses of the WENO scheme in acoustics include computational aeroacoustics and Mach stem formation.

TABLE I. Crest factor of input waveforms.

Waveform	Center frequency (Hz)	Crest factor (dB)
1	100	9.84
2	300	11.42
3	500	11.80

An input waveform was read into the algorithm with 200 points per wavelength at 20 kHz. Since the number of points per wavelength directly relates to the computation time, these parameters were chosen to allow for sufficient frequency resolution (related to points per wavelength) and propagation distance (related to the number of time steps by the Courant number) to allow for a reasonable amount of computation time. The WENO scheme's ability to propagate discontinuities also inherently includes an initial smoothing effect of the input waveform. The numerical smoothing for the input waveforms for the parameters previously stated alters the decay of the input spectrum at frequencies above approximately 2 kHz. Since the f^{-2} decay is necessary to have an initial haystack spectral shaped spectrum, the frequencies above 2 kHz are not shown. It must be noted that the WENO method does not have trouble creating frequencies above 2 kHz that occur with nonlinear distortion, but that the initial smoothing is the WENO scheme's attempt to ensure adequate smoothness of the broadband input waveform.

Three input waveforms were created using an array of 2^{16} Gaussian-distributed random numbers and filtered to have a haystack spectrum with center frequencies of 100, 300, and 500 Hz. The 100 Hz center frequency was chosen to be in the upper range of launch vehicles and the lower range of military jet aircraft while the 300 and 500 Hz center frequencies were chosen in the middle-to-high range of military jet aircraft. Center frequencies below 100 Hz become increasingly difficult to resolve temporally in terms of spectral density estimates for the computational and time resources available. The time series was scaled to have OASPL of approximately 165 dB, which is equivalent to a rms pressure just above 3.5 kPa.

The crest factor has been used to characterize the extreme-valued samples in rocket noise data to provide an indication of potential nonlinearity.[25] The crest factor, defined as

$$\mathrm{Cr} = 20\log\left(\frac{p_{\max}}{p_{\mathrm{rms}}}\right), \tag{9}$$

is shown for the input waveforms in Table I, revealing that the peak pressures are above 11.5 kPa (175 dB) for all three cases. As previously stated, the extreme pressures are more important than rms values in estimating nonlinearity. The crest factor for the waveforms used in the study approach the

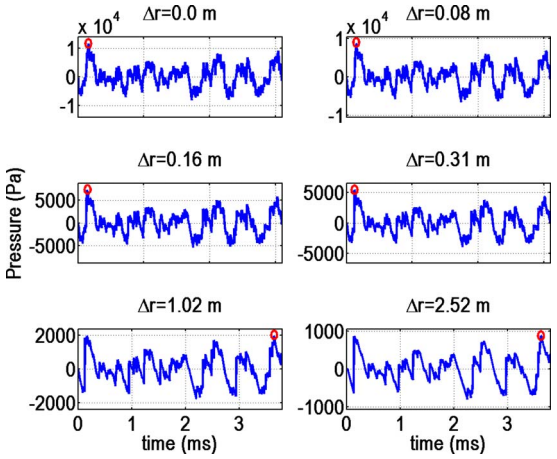

FIG. 1. (Color online) The first 30 000 points in the $f_c=100$ Hz waveform at six propagation distances. Nonlinear propagation has caused a shock to form after 0.31 m and shock coalescence to occur after 2.52 m. The maximum value (circled) changes peaks after 1.02 m.

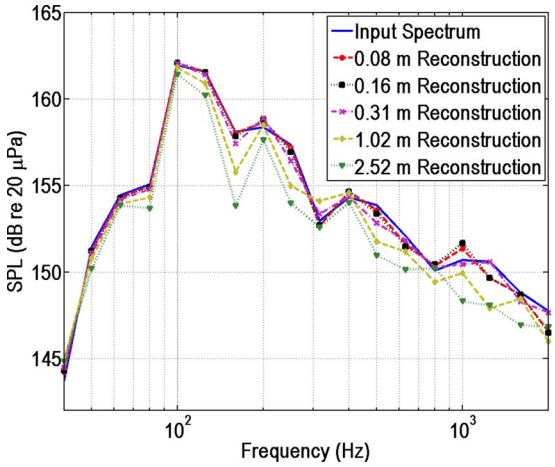

FIG. 2. (Color online) The reconstructed one-third octave spectra of the $f_c=100$ Hz waveform initially at 165 dB OASPL after propagating 0.08, 0.16, 0.31, 1.02, and 2.52 m along with the input spectrum at the source. Since the spectral shape is generally maintained despite the waveform steepening, the reconstructed spectra match the input spectra well.

valid limit for weak shock theory[33] but are handled correctly since the propagation algorithm is not based on weak shock theory.

The propagation was started 0.32 m from the spreading origin with absorbing boundary conditions to prevent numerical reflections. The waveforms were propagated 2.52 m, and the pressure waveform was sampled every 0.08 m. Because the propagation was one-dimensional, the linear reconstruction was performed by removing the $1/r$ magnitude decay due to the spherical spreading. This simple reconstruction scheme serves as a method to study the physics of the propagation, while estimating its effects on spectral characteristics over distance and the three center frequencies. For the remainder of this paper, the propagation distance (Δr) will be referenced from the propagation starting point, 0.32 m from the origin.

III. RESULTS

Figure 1 shows the first 30 000 points of the $f_c=100$ Hz waveform after propagating 0.08, 0.16, 0.31, 1.02, and 2.52 m. The maximum value in the waveform of 11.6 kPa is contained in this sample. Also displayed in Fig. 1 is the input time waveform to show the waveform's initial shape. Nonlinear propagation effects are clearly visible as portions of the waveform have become steepened, and the first shock forms from the maximum value after propagating 0.31 m. After 2.52 m, there is one main shock followed by a random set of steepened/shocked noise-fronts of smaller amplitude. Shock coalescence has clearly occurred after propagating 2.52 m as many of the higher frequency undulations/shocks have disappeared during the propagation. The energy from these frequencies has collected at the larger shock locations as a result of the nonlinear phase coupling. Also of note is that the peak value (circled in the figure) shifts from being at the beginning of the snapshot to a peak toward the end of the snapshot after 1.02 m.

The autospectrum of the $f_c=100$ Hz waveform was calculated, and the magnitude reconstruction back to the source location was applied. The original and reconstructed autospectra are compared on a one-third octave scale in Fig. 2. The reconstruction from 0.08, 0.15, and 0.31 m matches the source spectra very well, while the reconstruction from 1.02 and 2.52 m deviates slightly from the original spectrum. The deviations come from changes in the time waveform due to waveform steepening, but do not significantly affect the slope of the decay. This is because the energy transfer due to waveform steepening causes a high frequency roll-off proportional to f^{-2}, which the initial waveform already had. Additionally, the amplitude at the center frequency did not experience a shift in amplitude or frequency.

Figure 3 shows 20 000 points of the $f_c=300$ Hz waveform after propagating 0.08, 0.16, 0.31, 1.02, and 2.52 m along with the input time waveform. This set contains the waveform's maximum value of 11.7 kPa. The first shock forms after propagating 0.16 m. Shock coalescence has clearly occurred after 1.02 m of propagation, and the shocks appear to be interacting on a slightly larger scale than was seen in Fig. 1 so that when the waveform has reached

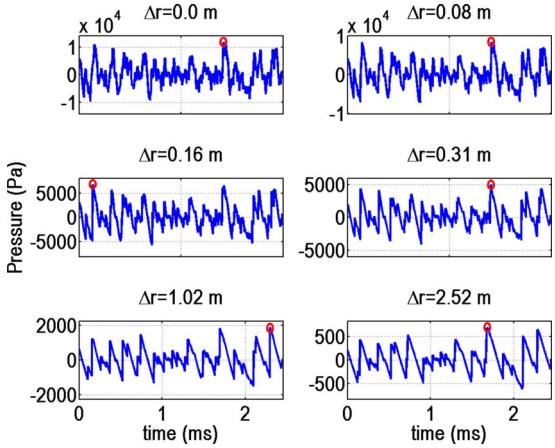

FIG. 3. (Color online) The first 20 000 points in the $f_c=300$ Hz waveform at six propagation distances. Nonlinear propagation has caused a shock to form after 0.16 m and shock coalescence to occur after 1.02 m. The maximum value (circled) changes peaks several times during the propagation.

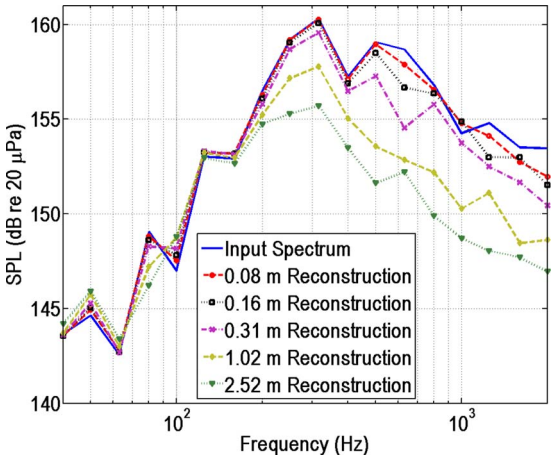

FIG. 4. (Color online) The reconstructed one-third octave spectra of f_c =300 Hz waveform initially at 165 dB OASPL after propagating 0.08, 0.16, 0.31, 1.02, and 2.52 m along with the input spectrum at the source. The amplitude of the center frequency drops for 1.02 and 2.52 m propagations due to energy transfer to high frequencies.

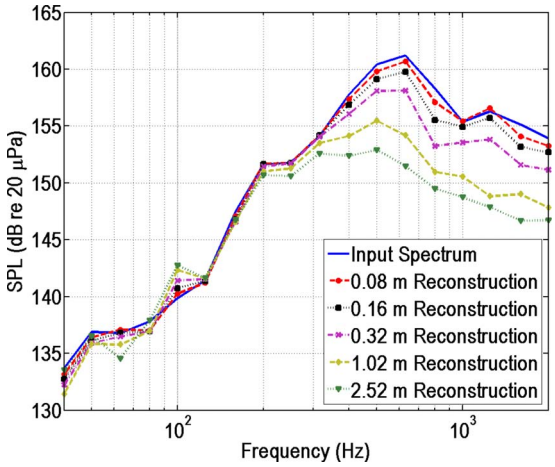

FIG. 6. (Color online) The reconstructed one-third octave spectra of f_c =500 Hz waveform initially at 165 dB OASPL after propagating 0.08, 0.16, 0.31, 1.02, and 2.52 m along with the input spectrum at the source. The amplitude of the center frequency drops in amplitude and frequency for 1.02 and 2.52 m propagations due to energy transfer high frequencies and loss in zero-crossings.

2.52 m, it consists of random arrays of shocks varying in amplitude. The waveform maximum value shifts peaks several times during the propagation.

The autospectrum of the f_c=300 Hz waveform was calculated, and the magnitude reconstruction back to the source location was applied, with the input and reconstructed autospectra compared on a one-third octave scale in Fig. 4. The reconstruction from 1.02 and 2.52 m deviates significantly from the input at and above the center frequency (300 Hz). The energy transfer from the center frequency to high frequencies was significant enough to cause the center frequency to drop almost 5 dB after 2.52 m. However, the center frequency does not shift downward.

The f_c=500 Hz waveform was also propagated out to the distance of 2.52 m at an initial OASPL of 165 dB, with the first 10 000 points shown in Fig. 5. A shock forms at the maximum value, initially at 12.3 kPa, after 0.08 m. Visual comparison reveals that the nonlinear distortion is significantly greater in Fig. 5 than in Fig. 1. This is to be expected

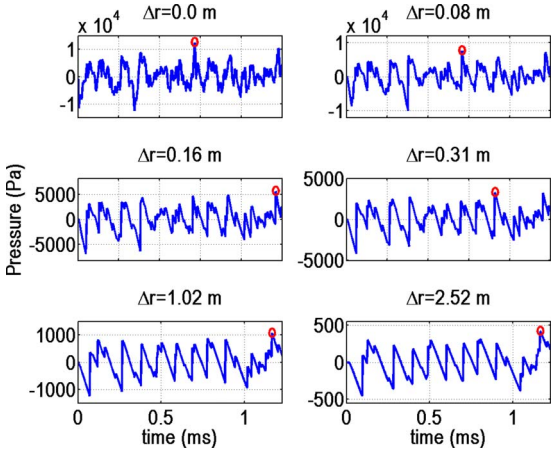

FIG. 5. (Color online) The first 10 000 points of the f_c=500 Hz waveform shown at six propagation distances. Nonlinear effects have caused shocks to form after 0.08 m and shock coalescence to occur by 1.02 m. The maximum value (circled) changes peaks several times during the propagation.

given the general trend that shock formation distance decreases as frequency increases. Shock coalescence is again evident after 1.02 m. After 2.52 m, the waveform is composed of nearly equispaced shocks of comparable amplitude and begins to partially resemble a sawtooth wave. The waveform maximum value has again shifted peaks several times during the propagation.

Figure 6 shows the reconstructed one-third octave spectra for the f_c=500 Hz waveform from the same distances shown previously. The center frequency amplitude begins to drop in amplitude after 0.08 m and begins to shift downward after 1.02 and 2.52 m. The downward shift in frequency is typically attributed to a decrease in zero-crossings as a result of the shock coalescence. The crest factor again shifts position during the propagation.

The overall sound pressure level is compared as a function of distance for all waveforms in Table II. After 2.52 m of linear propagation with spherical spreading, the OASPL for would be expected to drop 19 dB to the value of 146 dB. The f_c=100 Hz waveform has decayed 3 dB more than expected with spherical spreading alone, while the f_c=300 Hz

TABLE II. OASPL of the waveforms after propagating several distances compared to the levels resulting from just spherical spreading at those distances (rounded to the nearest decibel). Note that Δr is referenced to the propagation starting point and Δr+0.32 represents the distance from the origin.

Δr (m)	Spreading alone	100 Hz	300 Hz	500 Hz
0.00	165	165	165	165
0.08	163	163	163	163
0.16	162	162	161	160
0.31	159	159	158	157
1.02	153	152	150	148
2.52	146	145	142	139

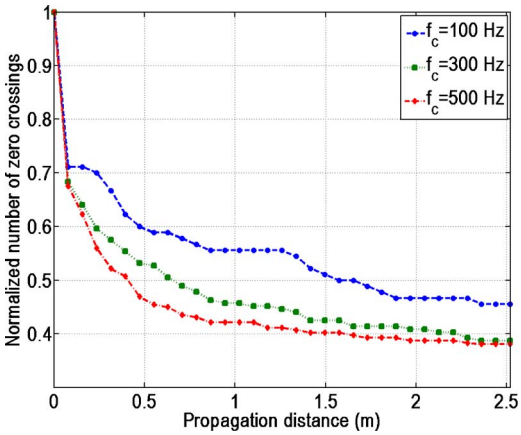

FIG. 7. (Color online) The number of zero-crossings normalized by the initial number of zero-crossing for all three waveforms. A decrease in the number of zero-crossings is shown for each waveform even though only the f_c=500 Hz waveform experiences a downward shift in center frequency (see Fig. 6).

and f_c=500 Hz waveforms have decayed 4 and 7 dB more, respectively. This discrepancy is a direct result of nonlinear shock attenuation.[24]

By visual inspection, all three waveforms involved at least some shock coalescence. For more thorough investigations of the existence of shock coalescence, technical metrics are typically used such as a decrease in the number of zero-crossings[34] or an increase in the characteristic time scale (which is inversely proportional to the center frequency).[19] However, for haystack-shaped noise, the center frequency dependence and random nature of the zero crossings make a direct comparison between the three case studies here impossible. Therefore, the number of zero-crossings normalized by their initial value is shown in Fig. 7 as a function of distance. All three waveforms share a decreasing trend in the number of zero-crossings as a function of propagation distance, with the f_c=100 Hz waveform having the lowest percentage of zero-crossings lost and the f_c=500 Hz having the highest. Since all three waveforms have a similar order of magnitude for the percent change in zero-crossings, but only the f_c=500 Hz waveform experienced a downward shift in frequency, this suggests that the percent change in zero-crossings alone does not give conclusive evidence of a downward frequency shift. Conversely, the absence of a downward shift in center frequency does not conclusively say that shock coalescence has not occurred.

In summary, for the same spectral shapes and OASPL but different center frequencies, the amount of nonlinear distortion is very different. This is expected since nonlinear effects occur over shorter distances for higher frequencies. The relatively good reconstruction for the f_c=100 Hz waveform indicates that although the time waveform changes, the spectral shape can generally be maintained despite the effects of nonlinearity. This occurs since the asymptotic dependence of low frequencies is proportional to f^2, and the high frequency roll-off resembles that of sawtooth wave spectrum, which decay according to the harmonic number.[19] This implies that haystack spectra may retain their spectral shape during magnitude reconstruction since the change in phase due to nonlinear coupling will not be detected. However, the results from the f_c=300 and 500 Hz waveforms indicate that when shock coalescence is more significant, the center frequency will shift downward and cause the high and low frequencies to be offset from the original spectrum, even though the high frequency slopes are similar.

For significant nonlinear propagation of waveforms with differing spectral shapes, the initial spectral shape would naturally not be retained. As shocks form, the nonlinearity will in essence filter the high and low frequency regions of the spectrum and cause significant changes in the spectral shape.[35]

IV. DISCUSSION

The results of this study have shown that shock coalescence can occur despite spherical spreading over short propagation distances near the spreading origin. Given these results, several observations will be discussed in a broader context.

First, the results presented above illustrate how important nonlinear behavior of haystack spectra will not be captured when studying spectrally white waveforms. The most obvious difference between the two is that the peak pressure levels of haystack spectra will be higher than a flat spectrum given the OASPL, therefore causing more nonlinear effects over shorter propagation distances. An effect entirely missed when studying spectrally white noise is how the center frequency influences the propagation, particularly how quickly the waveform will become random sawtooth waves. Comparison of Figs. 1 and 5 for propagation out to 2.52 m illustrates the significance of center frequency with respect to the waveform, transforming into a series of random sawtooth waves. Since the center frequency is partially dictated by the jet nozzle size and corresponding turbulence scales,[15] rocket noise typically has a lower center frequency in the jet noise. However, rocket noise levels are typically much higher than jet noise levels.

Next, several remarks must be made on the use of crest factors in nonlinear propagation of random noise of any spectral shape. As previously noted, McInerny[25] used the crest factor in analyses of rocket noise data to provide an indication of potential nonlinearity. However, Figs. 1, 3, and 5 show that the maximum value changes peaks during propagation. This illustrates how the maximum value is directly influenced by the behavior of the waveform samples directly preceding it. For example, a large negative pressure immediately prior to a large positive pressure will cause significant steepening to occur in both the positive and negative pressure regions, resulting in the formation of one large shock. The relative symmetry of the shock may cause the speed to be near the small amplitude sound speed [see Eq. (2)] while nonlinear attenuation will cause the amplitude to decay and lessen its long-term likelihood of overtaking other portions of the noise. Alternatively, if the large negative pressure was instead a large positive pressure, the shock speed, coalescence, and nonlinear attenuation would be completely different. Therefore, the crest factor is not necessarily a complete

metric for characterizing nonlinear propagation of noise. More detail on the suppression of large outliers due to shock attenuation is found in Ref. 19.

Finally, it has been noted how Pestorius and Blackstock[18] reasoned that spherical spreading will weaken nonlinear effects in the finite-amplitude propagation of noise so that energy transfer will be limited to high frequencies for most practical problems. Although this paper has clearly shown that substantial shock coalescence can occur over short propagation distances despite spherical spreading, a discussion of the assumptions made in this study is merited to determine whether this numerical experiment represents a practical problem.

Some reasoning suggests that the results from this experiment might represent an upper bound on the amount of nonlinearity that might occur near a military jet aircraft or launch vehicle. Center frequencies can be much lower than 500 or even 100 Hz, especially for noise caused by large rockets. This would result in larger propagation distances required for shock formation. Also, the extended nature of the source may cause superposing crossing waves to produce high levels without interacting long enough to produce cumulative nonlinear distortion. Additionally, partial source coherence and diffraction could prevent the waveform from developing shocks strong enough to rapidly coalesce near the source.

Despite these arguments, there are several factors which suggest that the results presented here may represent realistic amounts of nonlinearity near the finite-amplitude sources of interest. First, the amplitudes used in this study are comparable to the levels expected within several meters of military jet aircraft and launch vehicles. Second, the extended nature of the source will result in less than spherical decay near the plume, resulting in nonlinearity occurring relatively more quickly. Also, jet aircraft and rocket noise can exhibit significant positive skewness which, as mentioned previously, are due to large outliers. The higher number of large outliers will cause shock formation and coalescence more quickly than the Gaussian distribution presented here.

As a final point, there is relatively high coherence in the peak radiation direction of jet noise,[15,36] suggesting that the radiating waves from the large structures are not traveling in random directions. Because of this, waves propagating along this angle may have sufficient time for nonlinear interactions. Evidence supporting this idea has recently been observed in near-field, model-scale supersonic jet noise data,[37] where nonlinear effects were detected along the peak radiation direction. All of these arguments suggest that nonlinear interactions, including significant shock coalescence, can be expected within several meters of the plume region of military jet aircraft and rockets, specifically along the peak radiation angle.

V. CONCLUSION

This numerical experiment shows that nonlinear propagation effects can be significant enough to induce significant shock formation and coalescence in less than 3 m of propagation at amplitudes and center frequencies similar to those of military jet aircraft and rocket noise. Additionally, the center frequency of haystack spectra plays an important role in the amount of shock coalescence and how soon the waveform will transform into a series of random sawtooth waves. As previously discussed, arguments exist both for and against the likelihood of significant shock coalescence occurring in actual finite-amplitude jet or rocket noise. However, the results of this paper reveal the importance of seriously considering the finite-amplitude nature of jet or rocket noise sources in the near-field of the source. Furthermore, since nonlinear effects vary with amplitude, distance, and frequency, every source characterization technique performed on high-amplitude noise sources must carefully consider the relative importance of waveform steepening and shock formation before determining the accuracy of the results.

Since the exact role of shock coalescence in jet and rocket noise propagation is experimentally unverified, the results of this study suggest the need for further investigations that specifically target the existence and role of shock coalescence in the near-field of actual jet and rocket noise sources. Studies of the amount of shock coalescence required to appreciably alter a spectrum may help determine threshold sound pressure levels or distances for significant shock coalescence level. Statistics could be used to infer how characteristics of the noise change during propagation. Additionally, knowledge of the specific effects of shock coalescence and the scalability of shock formation and coalescence may help refine efforts in jet noise reduction and aid other advancements in vibroacoustic modeling of military aircraft and launch vehicles.

ACKNOWLEDGMENTS

The authors wish to gratefully acknowledge the financial support from NASA in collaboration with STI Technologies. Additionally, the authors thank Daniel Jensen and the Fulton Supercomputing Laboratory at Brigham Young University for computer support.

[1]J. N. Cole, H. E. von Gierke, D. T. Kyrazis, and A. J. Humphrey, "Noise radiation from fourteen types of rockets in the 1,000 to 130,000 pounds thrust range," WADC Technical Report No. 57-354 AD 130794, Wright Air Development Center, Wright-Patterson AFB, OH, 1957.
[2]W. H. Mayes, W. E. Lanford, and H. H. Hubard, "Near-field and far-field noise surveys of solid-fuel rocket engines of a range of nozzle exit pressures," NASA Technical Report No. TN D-21, NASA Langley RC, Langley Field, VA, 1959.
[3]R. C. Potter and M. J. Crocker, "Acoustic prediction methods for rocket engines, including the effects of clustered engines and deflected exhaust flow," NASA Report No. CR-566, NASA Marshall SFC, Huntsville, AL, 1966.
[4]R. C. Potter, "Noise field for shadowgraph model rocket experiments," NASA Report No. CR-76267, NASA, Washington, DC, 1966.
[5]R. C. Potter, "Investigation to locate the acoustic sources in a high speed jet exhaust stream," NASA Report No. CR-101105, NASA, Washington, DC, 1968.
[6]K. Eldred, "Acoustic loads generated by the propulsion system," NASA Technical Report No. SP-8072, Wyle Laboratories, NASA Langley RC, Hampton, VA, 1971.
[7]K. L. Gee, V. W. Sparrow, M. M. James, J. M. Downing, C. M. Hobbs, T. B. Gabrielson, and A. A. Atchley, "The role of nonlinear effects in the propagation of noise from high-power jet aircraft," J. Acoust. Soc. Am. **123**, 4082–4093 (2008).
[8]K. L. Gee, J. H. Giraud, J. D. Blotter, and S. D. Sommerfeldt, "Energy-

based acoustical measurements of rocket noise," AIAA Paper No. AIAA 2009-3165.
[9]R. H. Schlinker, S. A. Liljenberg, D. R. Polak, K. A. Post, C. T. Chipman, and A. M. Stern, "Supersonic jet noise source characteristics propagation: Engine and model scale," AIAA Paper No. AIAA 2007-3623.
[10]R. J. Kenny, C. Hobbs, K. Plotkins, and D. Pilkey, "Measurement and characterization of space shuttle solid rocket motor plume acoustics," AIAA Paper No. AIAA 2009-3161.
[11]S. Saxena, P. J. Morris, and K. Viswanathan, "Algorithm for the nonlinear propagation of broadband jet noise," AIAA J. **47**, 186–194 (2009).
[12]M. Kandula, "Near-field acoustics of clustered rocket engines," J. Sound Vib. **309**, 852–857 (2008).
[13]D. Casalino, M. Barbarino, M. Genito, and V. Ferrara, "Hybrid empirical/computational aeroacoustic methodology for rocket noise modeling," AIAA J. **47**, 1445–1460 (2009).
[14]C. K. W. Tam, N. N. Pastouchenko, and R. H. Schlinker, "Noise source distribution in supersonic jets," J. Sound Vib. **291**, 192–201 (2006).
[15]C. K. W. Tam, K. Viswanathan, K. K. Ahuja, and J. Panda, "The sources of jet noise: Experimental evidence," AIAA Paper No. AIAA 2007-3641.
[16]C. L. Morfey and G. P. Howell, "Nonlinear propagation of aircraft noise in the atmosphere," AIAA J. **19**, 986–992 (1981).
[17]S. A. McInerny and S. M. Ölçmen, "High-intensity rocket noise: Nonlinear propagation, atmospheric absorption, and characterization," J. Acoust. Soc. Am. **117**, 578–591 (2005).
[18]F. M. Pestorius and D. T. Blackstock, "Experimental and theoretical study of propagation of finite-amplitude noise in a pipe," in *Finite-Amplitude Wave Effects in Fluids*, edited by L. Bjorno (IPC Science and Technology Press, Ltd., Guildford, UK, 1973).
[19]S. N. Gurbatov and O. V. Rudenko, "Statistical phenomena," in *Nonlinear Acoustics*, edited by M. F. Hamilton and D. T. Blackstock (Academic Press, San Diego, CA, 1998).
[20]V. W. Sparrow and R. Raspet, "A numerical method for general finite amplitude wave propagation in two dimensions and its application to spark pulses," J. Acoust. Soc. Am. **90**, 2683–2691 (1991).
[21]T. Yano and Y. Inoue, "Numerical study of strongly nonlinear acoustic waves, shock waves and streaming caused by a harmonically pulsating sphere," Phys. Fluids **6**, 2831–2844 (1994).
[22]Y. Jing and R. O. Cleveland, "Modeling the propagation of nonlinear three-dimensional acoustic beams in homogeneous media," J. Acoust. Soc. Am. **122**, 1352–1364 (2007).
[23]D. T. Blackstock, "Nonlinear propagation in jet noise," in *Proceedings of the 3rd Interagency Symposium on University Research in Transportation Noise* (University of Utah, Salt Lake City, UT, 1975), pp. 389–397.
[24]D. T. Blackstock, M. F. Hamilton, and A. D. Pierce, "Progressive waves in lossless and lossy fluids," in *Nonlinear Acoustics*, edited by M. F. Hamilton and D. T. Blackstock (Academic Press, San Diego, CA, 1998).
[25]S. A. McInerny, "Launch vehicle acoustics Part 2: Statistics of the time domain data," J. Aircr. **33**, 518–523 (1996).
[26]B. P. Petitjean, K. Viswanathan, and D. K. McLaughlin, "Acoustic pressure waveforms measured in high speed jet noise experiencing nonlinear propagation," AIAA Paper No. AIAA 2005-209.
[27]K. L. Gee, V. W. Sparrow, A. A. Atchley, and T. B. Gabrielson, "On the perception of crackle in high-amplitude jet noise," AIAA J. **45**, 593–598 (2007).
[28]J. Lighthill, "The inaugural theodorsen lecture: Some aspects of the aeroacoustics of high-speed jets," Theor. Comput. Fluid Dyn. **6**, 261–280 (1994).
[29]V. A. Khokhlova, O. V. Rudenko, and O. A. Sapozhnikov, "Sawtooth waves: One dimensional statistical ensembles and thermal self-focusing of the beam," in *Frontiers of Nonlinear Acoustics: Proceedings of the 12th ISNA*, edited by M. F. Hamilton and D. T. Blackstock (Elsevier Science Publications, Ltd., London, UK, 1990).
[30]M. S. Wochner, "Numerical simulation of multi-dimensional acousitc propagation in air including the effects of molecular relaxation," Ph.D. thesis, The Pennsylvania State University, University Park, PA (2006).
[31]M. S. Wochner, A. A. Atchley, and V. W. Sparrow, "Numerical simulation of finite amplitude wave propagation in air using a realistic atmospheric absorption model," J. Acoust. Soc. Am. **118**, 2891–2898 (2005).
[32]C. W. Shu, "Essentially non-oscillatory and weighted essentially non-oscillatory schemes for hyperbolic conservation laws," in *Advanced Numerical Approximation of Nonlinear Hyperbolic Equations*, edited by A. Quarteroni (Springer, Berlin, Germany, 1998).
[33]F. M. Pestorius and S. B. Williams, "Upper limit on the use of weak-shock theory," J. Acoust. Soc. Am. **55**, 1334–1335 (1974).
[34]B. P. Petitjean and D. K. McLaughlin, "Experiments on the nonlinear propagation of noise from supersonic jets," AIAA Paper No. AIAA 2003-3127.
[35]M. R. Shepherd, "The effects of nonlinear propagation on near-field acoustical holography," MS thesis, Brigham Young University, Provo, UT (2007).
[36]K. Viswanathan, "Investigation of the sources of jet noise," AIAA Paper No. AIAA 2007-3601.
[37]K. L. Gee, M. R. Shepherd, L. E. Falco, A. A. Atchley, L. S. Ukeiley, B. J. Jansen, and J. M. Seiner, "Identification of nonlinear and near-field effects in jet noise using nonlinearity indicators," AIAA Paper No. AIAA 2007-3653.